THE JOURNAL OF PHYSICAL CHEMISTRY C
A JOURNAL OF THE AMERICAN CHEMICAL SOCIETY

pubs.acs.org/JPCC

Article

Mechanistic Study of Seed-Mediated Growth of Gold Rhombic Dodecahedra

Published as part of The Journal of Physical Chemistry virtual special issue "Marie-Paule Pileni Festschrift".

Xiaohuan Zhao,[¶] Veronica D. Pawlik,[¶] Da Huo, Shan Zhou, Bai Yang, and Younan Xia*

Cite This: *J. Phys. Chem. C* 2021, 125, 27394–27402

Read Online

ACCESS | Metrics & More | Article Recommendations | Supporting Information

ABSTRACT: It is a viable approach to tailor the optical and catalytic properties of noble-metal nanocrystals by controlling their geometric shapes. Among various shapes, rhombic dodecahedra are considered particularly difficult to synthesize owing to the higher energy of {110} facets relative to other low-index facets. Here we report a facile synthesis of Au rhombic dodecahedra with high uniformity and purity through seed-mediated growth in *N*,*N*-dimethylformamide (DMF) containing a small amount of water. The success of this synthesis critically relied on the use of single-crystal seeds with a spherical shape, the capability of DMF to selectively cap the {110} facets, and the balance between deposition and surface diffusion. We systematically investigated the effects of the amounts of poly(vinylpyrrolidone) (PVP), seeds, and water on the synthesis, as well as reaction temperature and time. Under the condition optimal for layer-by-layer growth and with the use of 10 nm seeds, the edge lengths of the rhombic dodecahedra could be tuned from 18−36 nm by increasing the duration of growth time. This method also offers a facile route to Au nanocrystals with other shapes. For example, by varying the amount and molecular weight of PVP, as well as temperature, the same protocol could be adapted to obtain trisoctahedra and octahedra, respectively, in high yield and quality.

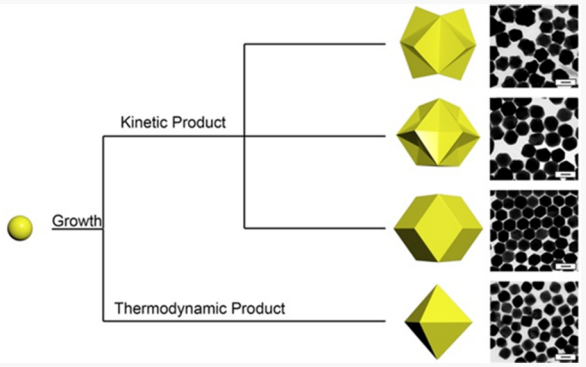

INTRODUCTION

Gold (Au) nanocrystals have received tremendous attention over the past several decades. Their fascinating properties, such as localized surface plasmon resonance (LSPR),[1] excellent biocompatibility,[2] easy and robust surface modification,[3] and catalytic activity,[4] have enabled their use in catalysis,[4] sensing,[5] photonics,[6] electronics,[7] and biomedicine.[8] Since the optical, electronic, and catalytic properties of nanocrystals are strongly correlated with their shape and size,[9] it is vital to optimize their use in various applications by gaining tight controls over these parameters. In this regard, a great deal of efforts has been devoted to the colloidal synthesis of Au nanocrystals with well-defined and controllable shapes and sizes.

In terms of shape control, Au nanocrystals have been prepared with diverse morphologies, including spheres, cubes, octahedra, decahedra, icosahedra, rods, and plates.[9−11] Essentially, most of these nanocrystals are enclosed by a mix of {111} and {100} facets in various proportions. For a face-centered cubic (*fcc*) metal, these two facets possess relatively low surface energies, making them more favorable in terms of thermodynamics. It is generally accepted that metal atoms tend to be deposited onto the facets high in surface free energy to help minimize the total surface free energy.[12] For this reason, it is not difficult to understand why it has been particularly challenging to synthesize nanocrystals enclosed by {110} facets, which possess the highest surface energy among the low-index facets.

Compared to other shapes, there are only a limited number of reports on the synthesis of Au rhombic dodecahedra (AuRD) because their surfaces are enclosed by {110} facets. The synthetic approaches can be divided into two major categories: one-pot and seed-mediated growth. The one-pot synthesis of AuRD typically involves *N*,*N*-dimethylformamide (DMF) and/or water as the solvent and reductant while a polyol method has also been reported.[13−15] Specifically, Han et al. synthesized AuRD through direct reduction of $HAuCl_4$ by pure DMF at 90−95 °C for 15 h without introducing additional reductant and capping agent.[13] The AuRD had a broad distribution in size, which could be tuned neither larger nor smaller. Park et al. reduced $HAuCl_4$ in a mixture of DMF and water (7.5:1 by vol.) at 120 °C for 2 h in the presence of poly(vinylpyrrolidone) (PVP).[14] In this case, however, AuRD

Received: September 20, 2021
Revised: November 17, 2021
Published: December 1, 2021

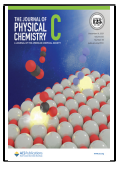

https://doi.org/10.1021/acs.jpcc.1c08288
J. Phys. Chem. C 2021, 125, 27394−27402

were only observed in the very early stage of the synthesis as they quickly transitioned into octahedra within 8 min. Zhou et al. also reported a one-pot synthesis involving the use of ethylene glycol (EG) as a reductant and poly(diallyldimethylammonium) chloride (PDDA) as a coordination ligand, but the AuRD were not formed directly.[15] Instead, octahedra were formed first and then transformed into AuRD by carefully manipulating the temperature to adjust the reducing power of EG. In addition, the Cl^- from $AuCl_4^-$ and PDDA could be combined with the O_2 from air to slowly etch the octahedra to generate facets higher in energy than {111} while the underpotential deposition of Ag^+ ions could help stabilize the newly exposed {110} facets. The as-obtained AuRD had an edge length of about 100 nm.

Most of the reported syntheses are based on seed-mediated growth,[16−21] and they can be further divided into two categories with regard to the reaction medium: water versus a mixture of DMF and water. Using an aqueous system, Niu et al. successfully synthesized spherical Au seeds using ascorbic acid (AA) as a reducing agent and cetylpyridinium chloride (CPC) as a capping agent.[16] The CPC-capped Au nanospheres with an average diameter of 41.3 nm were then used as seeds for the subsequent growth of AuRD in an aqueous solution at 30 °C for 2 h. The resultant AuRD had a relatively high purity. However, their sizes could not be tuned nor did their surfaces show well-defined {110} facets either. Huang et al. also successfully synthesized AuRD in an aqueous system through seed-mediated growth of 3−5 nm Au nanospheres in the presence of either NaBr or KI.[17,18] By adjusting the amount of the seeds, the size of the as-obtained AuRD could be tuned from 37−74 nm. It is worth noting that the shape evolution from cubes to trisoctahedra and RD could be successfully achieved by varying the amount of AA while using cetyltrimethylammonium chloride (CTAC) and NaBr as the capping agents.[17] When using CTAC and KI, the shape evolution from RD to octahedra could be achieved by varying the amount of KI.[18] More recently, Huang et al. revisited the seed-mediated synthesis in an aqueous solution, but this time with a focus on the manipulation of Au(III) precursor amount and a closer look at the role played by CTAC.[19] By changing the volume of Au(III) precursor added while keeping all other components fixed, it was possible to tune the reaction cell potential, which is an important component of the Nernst equation that governs the reaction. Interestingly, replacing CTAC with NaCl did not result in the same shape control, indicating that the complexation of the CTA^+ component with the Au(III) precursor was more important to shape control than any capping effect that Cl^- might provide. However, except for the acknowledgment that this method subtly alters the redox chemistry to transform octahedra into RD and that halides do not contribute to shape control, there is still no explanation for the formation or retention of {110} facets. In a water-based synthesis of Au nanocrystals, Mirkin et al. also observed the formation of RD albeit the sample suffered from the presence of a large proportion of bipyramids as the byproduct.[20] Additionally, seed-mediated synthesis was conducted in a mixture of DMF and water. In a demonstration by Park et al., AuRD with an edge length in the range of 19−67 nm were obtained by conducting the synthesis at 70 °C for 3 h, with PVP and trisodium citrate serving as the capping agents.[21] However, the products were not perfect RD. Their protruded vertices indicated that the as-prepared AuRD were enclosed by a mix of {110} and its vicinal facets on the surface.

Herein, we report a seed-mediated synthesis of AuRD with a narrow size distribution and high purity by conducting the growth in DMF mixed with a trace amount of water (171:1 by volume). The products showed well-defined {110} facets and nonprotruding vertices. In contrast to previously reported methods, which relied on the reducing power of DMF or EG, we used PVP at a high concentration to leverage its reducing power. The introduction of PVP not only accelerated the reduction kinetics but also significantly narrowed the size distribution of the particles. By varying the amount and molecular weight of PVP, we established that the hydroxyl groups on the ends of PVP were critical to its reducing power. We systematically investigated the effects of the amounts of PVP, seeds, and water on the synthesis, as well as reaction temperature, to identify the optimal condition for achieving layer-by-layer growth. With the use of 10 nm spherical seeds, the edge lengths of the AuRD could be tuned from 18−36 nm by allowing the growth to proceed for different periods of time under the condition optimal for layer-by-layer growth. We further demonstrated that, by adjustment of the experimental parameters, the same protocol could be used to obtain Au nanocrystals with other morphologies, including octahedra and trisoctahedra.

EXPERIMENTAL SECTION

Materials. Tetrachloroauric(III) acid ($HAuCl_4 \cdot 3H_2O$, ≥ 99.0%), *N*,*N*-dimethylformamide (DMF, ≥99%), sodium borohydride ($NaBH_4$, ≥99%), L-ascorbic acid (AA, >99%), poly(vinylpyrrolidone) (PVP, MW ≈ 55 000), hexadecyltrimethylammonium bromide (CTAB, ≥99%), and hexadecyltrimethylammonium chloride (CTAC, 25% wt/vol. aqueous solution) were all obtained from Sigma-Aldrich (St Louis, MO) and used as received. Deionized water with a resistivity of 18.2 MΩ·cm was used throughout the experiments.

Synthesis of the Au Spherical Seeds. The Au spherical seeds were synthesized as previously reported.[21] Initially, Au clusters were prepared by adding 0.6 mL of a 10 mM $NaBH_4$ aqueous solution to 10 mL of a 0.25 mM $HAuCl_4$ and 0.1 M CTAB aqueous solution. The mixture was shaken gently for 2 min, and then it was kept undisturbed at 27 °C for 3 h to ensure the complete decomposition of excess $NaBH_4$. Afterward, in a separate 20 mL glass vial, 1.5 mL of 0.1 M AA, 4 mL of 0.25 mM $HAuCl_4$, and 4 mL of 0.1 mM CTAC were combined before adding 0.1 mL of the as-prepared Au clusters. This reaction was allowed to proceed for 1 h, after which the solid products were collected via centrifugation at 14500 rpm for 30 min and then washed with water. The as-obtained Au nanospheres with a mean diameter of approximately 10 nm was redispersed in water to reach a final concentration of 10.66 mg/mL as confirmed by inductively coupled plasma mass spectrometry (ICP-MS).

Synthesis of Au Rhombic Dodecahedra. In a standard synthesis, 6 mL of DMF, 200 mg of PVP (MW ≈ 55 000), 10 μL of the 10 nm Au seeds, and 25 μL of 40 mM $HAuCl_4$ were mixed in a 20 mL glass vial at room temperature. The vial was capped and heated at 90 °C under magnetic stirring for 60 min and then immersed in ice-cold water to quench the reaction. The solid product was then collected via centrifugation at 14000 rpm for 5 min and washed three times with water. Finally, the product was redispersed in water for further characterizations. To investigate the influence of water during the reaction, DMF was partially replaced with water while keeping the total volume unchanged.

https://doi.org/10.1021/acs.jpcc.1c08288
J. Phys. Chem. C 2021, 125, 27394−27402

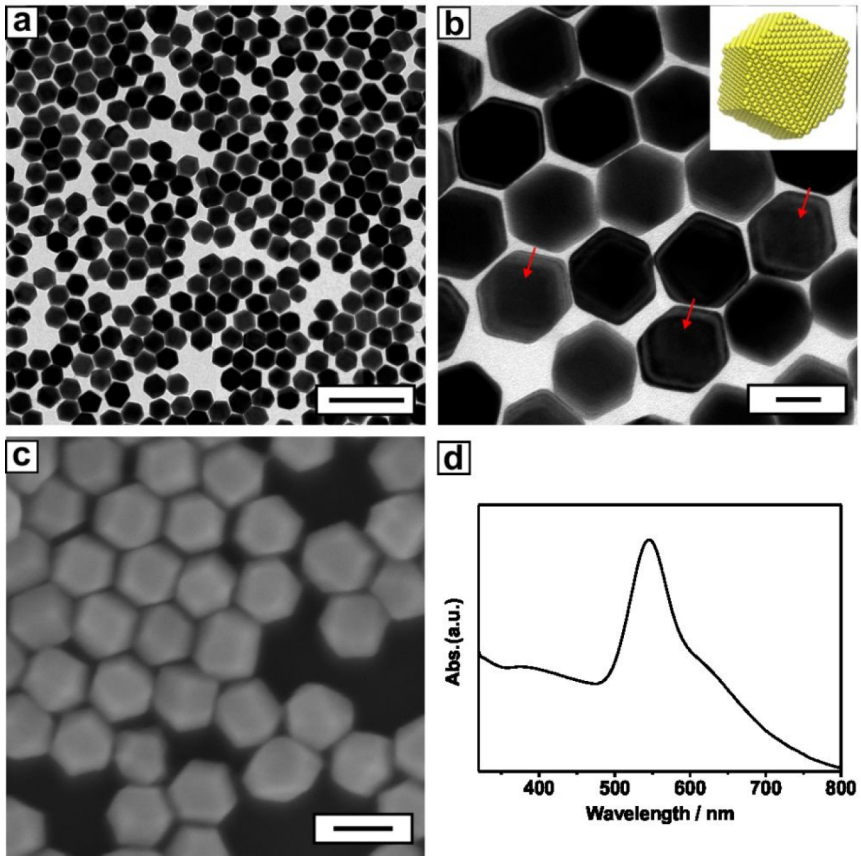

Figure 1. (a) Low- and (b) high-magnification TEM images of the AuRD prepared using the standard protocol. The scale bars are 200 and 30 nm for parts a and b, respectively. The red arrows in part b indicate three RD projected along ⟨110⟩ direction, together with an atomic model oriented along the same direction. (c) SEM image of the AuRD from the same batch of sample prepared using the standard protocol (scale bar: 50 nm). (d) UV−vis spectrum recorded from an aqueous suspension of the AuRD.

Characterizations. The SEM images were recorded using a field-emission microscope (Adobe Acrobat X Pro, ADOBE) operated at an accelerating voltage of 20 kV. The TEM images were captured on an electron microscope (JEOL-1400, Jeol) operated at an accelerating voltage of 120 kV. The samples were prepared by placing a few drops of the colloidal suspension in water either on silicon substrates for SEM or on copper grids coated with carbon for TEM. The UV/vis spectra were recorded with a spectrometer (Cary 60, Agilent) with the particles suspended in water. The concentration of Au was determined by ICP-MS (NexION 300Q, PerkinElmer). The sample for ICP-MS was prepared by dissolving the Au particles in a mixture of hydrochloric acid (HCl, 37% in volume, 0.3 mL) and nitric acid (HNO_3, 70% in volume, 0.1 mL), followed by dilution with water (9.6 mL).

RESULTS AND DISCUSSION

The synthesis of AuRD can be divided into three steps. In the first two steps, single-crystal Au seeds with a spherical shape were prepared by following a reported protocol, which involved quick reduction of $HAuCl_4$ by $NaBH_4$ in the presence of hexadecyltrimethylammonium bromide (CTAB). The clusters produced in the first step were then grown into spherical seeds of ca. 10 nm in diameter by reducing a proper amount of $HAuCl_4$ with ascorbic acid (AA) in the presence of hexadecyltrimethylammonium chloride (CTAC).[22] In the third step, the spherical seeds were grown into AuRD through the addition of more $HAuCl_4$ in the presence of PVP, DMF, and a trace amount of water. Figure 1a shows a transmission electron microscopy (TEM) image of the solid products obtained using the standard protocol. The particles were uniform in terms of both size and shape, with an average edge length of ca. 31 nm and purity >90%. The particles indicated by red arrows in Figure 1b were all projected along the ⟨110⟩ direction. The inset provides an atomic model oriented along the same direction. Figure 1c shows a scanning electron microscopy (SEM) image of the same sample, confirming the rhombic dodecahedral shape while demonstrating the uniformity in terms of both size and shape. Finally, Figure 1d shows a typical UV−vis spectrum recorded from an aqueous suspension of the AuRD, presenting a major LSPR peak positioned at 547 nm, together with a shoulder peak at a longer wavelength.

To shed light on the growth mechanism of the AuRD, we analyzed the samples collected at different time points of a standard synthesis. Parts a and b of Figure 2 show TEM images of the particles obtained at t = 30 and 45 min, respectively. The products were dominated by AuRD with edge lengths of 18 and 26 nm, respectively, albeit the growth of the spherical seeds was somewhat stunted as a result of the shortened reaction time relative to the sample shown in Figure 1 (t = 60 min). Closer inspection of the TEM images reveals shape irregularity arising from insufficient atom deposition, preventing complete evolution of the spherical seeds into AuRD. When the duration of growth was extended to 120 and 240 min, we obtained AuRD with edge lengths of 33 and 36 nm,

https://doi.org/10.1021/acs.jpcc.1c08288
J. Phys. Chem. C 2021, 125, 27394−27402

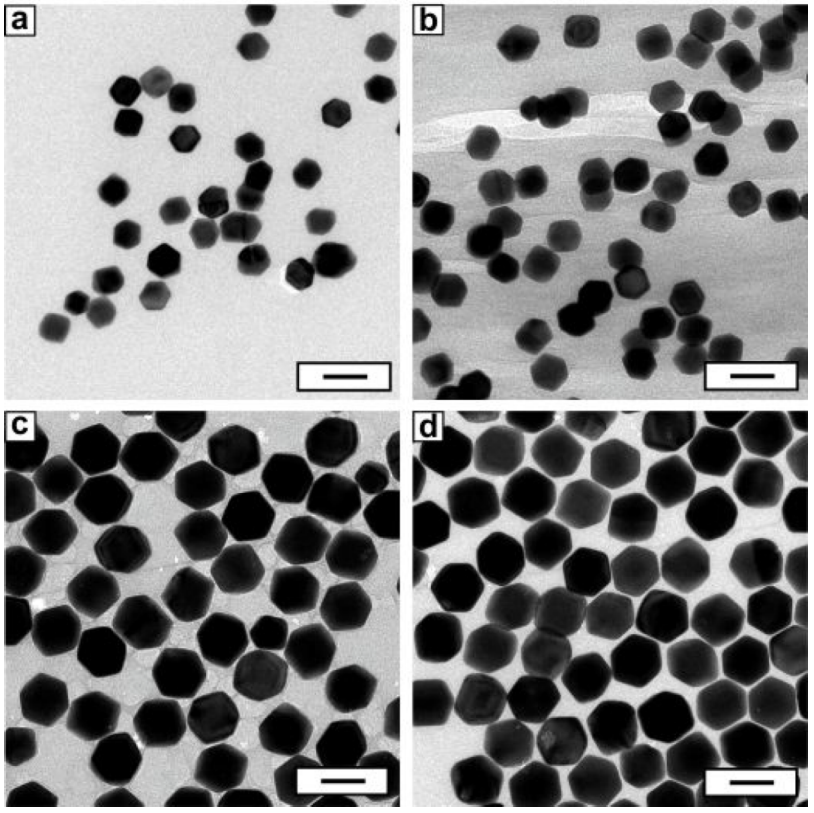

Figure 2. TEM images of the Au nanocrystals synthesized using the standard protocol except for the variation of reaction time from 60 min to (a) 30, (b) 45, (c) 120, and (d) 240 min, respectively. Scale bars: 50 nm.

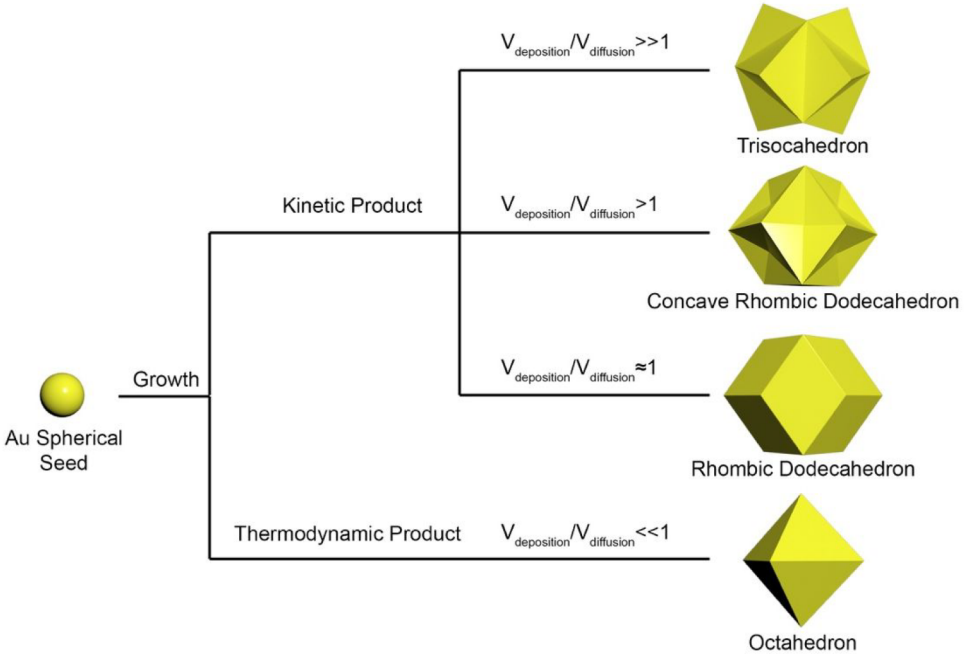

Figure 3. Experimental conditions that lead to the formation of rhombic dodecahedra of different sizes, trisoctahedra, and octahedra, from the same batch of spherical seeds.

respectively. The TEM images in parts c and d of Figure 2 clearly show the enlargement in particle size as the growth time was prolonged. The gradual increase in edge length from 18 to 36 nm as a function of growth time, together with a narrow size distribution, suggests the involvement of layer-by-layer growth, which is different from the mechanism reported in a prior study.[14]

Figure 3 shows a schematic of the mechanism proposed to account for the growth process. Because the {110} facets on the spherical seeds are supposed to be selectively capped by

https://doi.org/10.1021/acs.jpcc.1c08288
J. Phys. Chem. C 2021, 125, 27394−27402

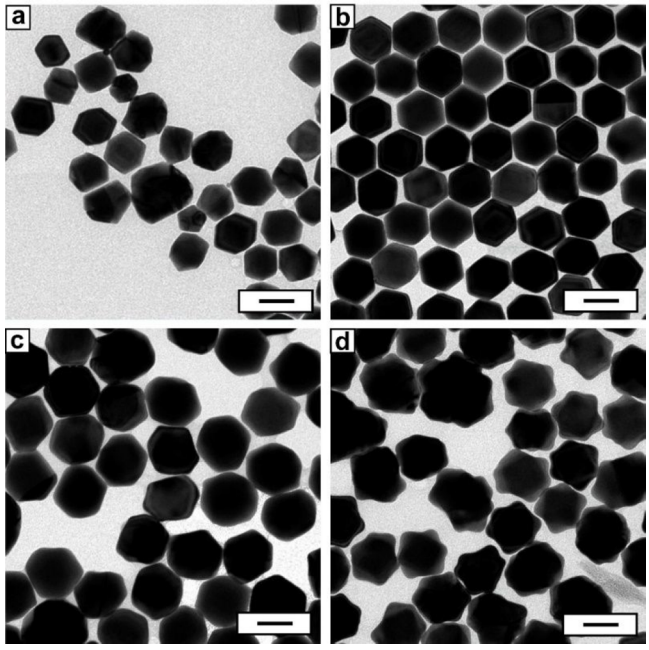

Figure 4. TEM images of the Au nanocrystals synthesized using the standard protocol except that the amount of PVP was changed from 200 mg to (a) 100, (b) 150, (c) 300, and (d) 400 mg, respectively. Scale bars: 50 nm.

DMF (or one of its oxidation products),[13] the newly formed Au atoms should be preferentially deposited onto other facets, transforming the seeds into AuRD. Corresponding to a spherical seed of 10 nm in diameter, the smallest RD was estimated to be approximately 12 nm in edge length. Afterward, the corners and edges on the RD can keep receiving additional Au atoms to continue the growth process. If the newly deposited Au atoms are able to diffuse to and cover the side faces terminated in {110} facets, AuRD with gradually enlarged sizes will be obtained through a layer-by-layer growth mechanism. Otherwise, the atoms would be accumulated on the corners and edges for the creation of concave side faces. Depending on the deposition rate relative to the surface diffusion rate, the just-formed AuRD will evolve into RD with concave faces, regular RD with enlarged sides, and trisoctahedra, respectively, as the growth is continued. In the case of extremely slow deposition relative to surface diffusion, the spherical seeds would grow into octahedra, a shape most favorable in terms of thermodynamics. Taken together, AuRD can only be obtained in the presence of an effective capping agent for the {110} facets and under the experimental condition optimal for layer-by-layer growth.

We argue that PVP should be able to serve the dual roles as both a colloidal stabilizer and a reducing agent in the present synthesis.[23] A similar synthesis involving no PVP required a much longer reaction time of 15 h to obtain AuRD and the product was compromised by a broader size distribution.[13] To systematically evaluate the effect of PVP, we varied the amount of PVP added into the reaction solution while keeping all other parameters the same as those in the standard protocol. Figure 4a shows a TEM image of the particles obtained in the presence of 100 mg of PVP. The nanocrystals lacked uniformity in terms of size and shape, suggesting that the

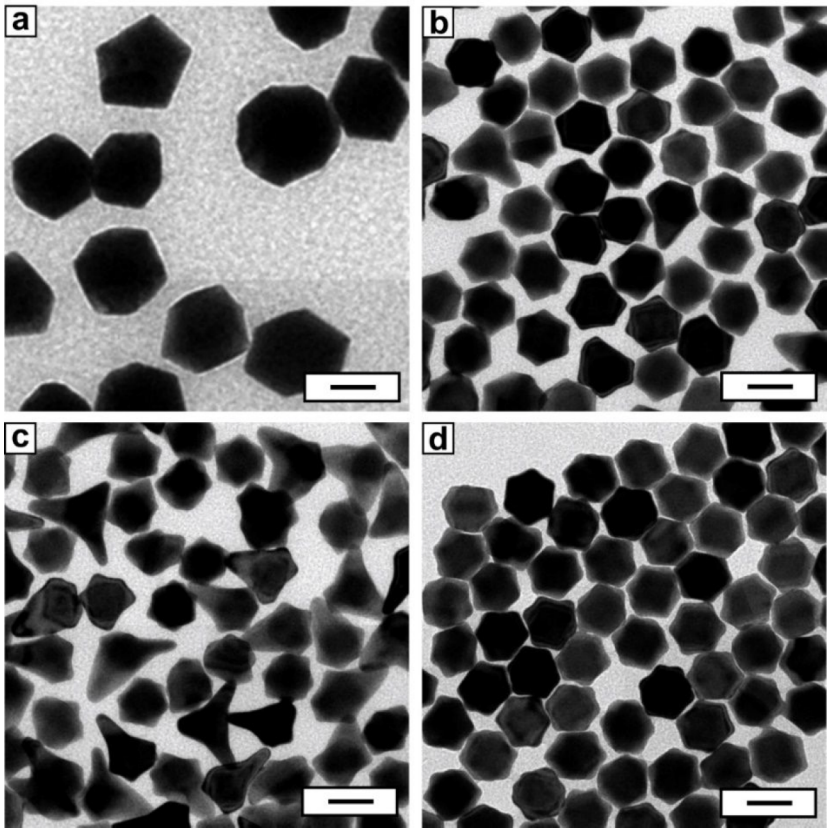

Figure 5. TEM images of the Au nanocrystals synthesized using the standard protocol except for the use of PVP with different molecular weights of (a) 360 000, (b) 40 000, (c) 20 000, and (d) 10 000, respectively, rather than 55 000. Scale bars: 50 nm.

https://doi.org/10.1021/acs.jpcc.1c08288
J. Phys. Chem. C 2021, 125, 27394−27402

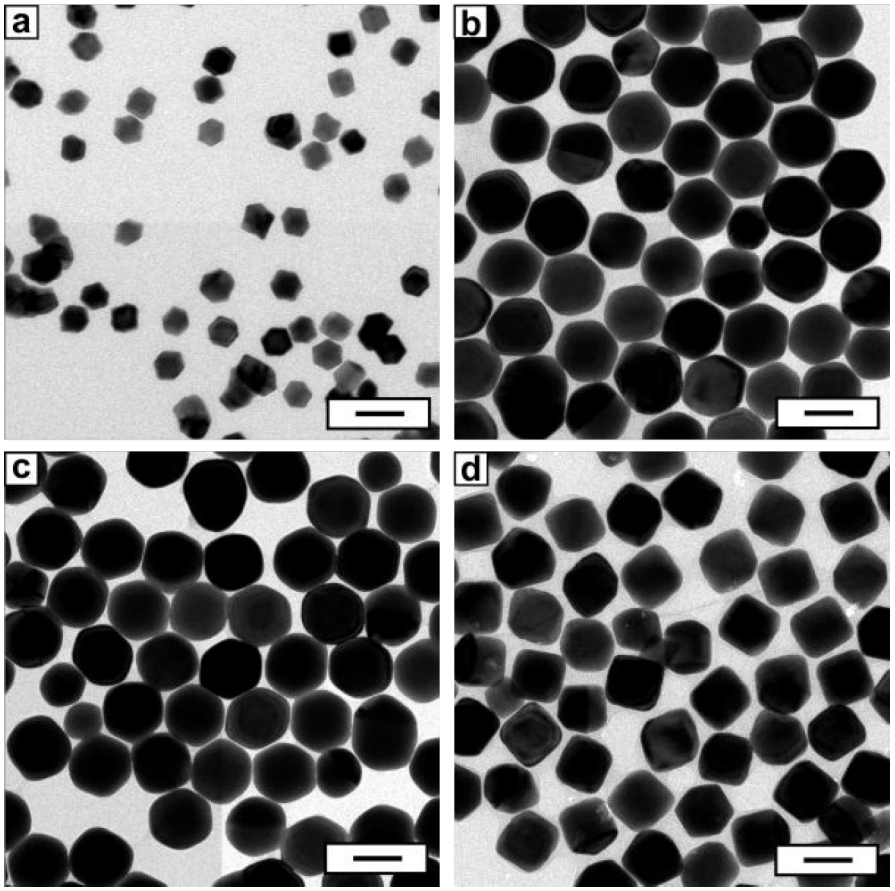

Figure 6. TEM images of the Au nanocrystals synthesized using the standard protocol except that the reaction temperature was changed from 90 °C to (a) 70, (b) 110, (c) 130, and (d) 150 °C, respectively. Scale bars: 50 nm.

growth was yet to be completed after 60 min. This trend is consistent with the retarded reaction kinetics observed in a synthesis involving no PVP.[13] When the amount of PVP was increased to 150 mg, the reduction kinetics was accelerated, leading to the formation of AuRD with a uniform shape and a narrow size distribution (Figure 4b). When the amount of PVP was further increased to 300 and 400 mg, the deposition rate began to outpace the diffusion rate, allowing atoms to accumulate on the sites not capped by DMF, such as corners and edges for the generation of concave side faces,[24] as shown in Figure 4c. When the deposition became too fast relative to surface diffusion, the significant increase in concavity for the side faces of AuRD eventually led to the formation of trisoctahedral nanocrystals (Figure 4d). As shown by the UV−vis spectrum in Figure S1, the LSPR peak of the Au trisoctahedral nanocrystals was slightly red-shifted relative to that of the AuRD.

Another parameter that directly affects the reduction power of PVP is its molecular weight or the proportion of end groups. Samples synthesized using PVP with a higher molecular weight of 360 000 resulted in nanocrystals that were once again bigger and less uniform in both shape and size, indicating compromise in terms of reduction power (Figure 5a). This trend continued in PVPs with lower molecular weights of 40 000, 20 000, and 10 000 for their gradual enhancement in reduction power. Parts b−d of Figure 5 show obvious overgrowth on the corners and edges (some or all of them) of the AuRD, indicating that a faster reduction rate promoted deposition over diffusion. The results in Figures 4d and 5d demonstrate that preferential overgrowth at the corners and edges of AuRD can also be used to generate trisoctahedra featuring a narrow size distribution and uniform shape. Taken together, increasing the amount of PVP and reducing the molecular weight of PVP both gave the same result, pointing toward the important role of the concentration of the hydroxyl end groups in determining the reduction kinetics.

We also varied the temperature from 70 to 150 °C to explore the thermodynamic and kinetic aspects of the synthesis. At 70 °C, the synthesis resulted in smaller and concave AuRD. Because the actual amount of precursor used in the synthesis did not change, the smaller size indicated that there was insufficient reduction at such a low temperature (Figure 6a). The concavity of the side faces was a manifestation of the inadequate surface diffusion for the deposited atoms. At higher temperatures of 110 and 130 °C, the rhombic dodecahedra moved past their regular shape and began to look more spherical as their side faces became more convex (Figure 6, parts b and c). The rise in temperature suggests weakened adsorption of DMF, which was supposed to act as a selective capping agent toward the {100} facets, gradually making the expression of such high-energy facets on the nanocrystals less favorable. As a result, Au atoms could be directly deposited on or readily transported to the {110} facets through surface diffusion, leading to the formation of facets other than {110}. When the temperature was further increased to 150 °C, DMF completely lost its ability to serve as a capping agent while atomic deposition on the {110} facets became dominant over other facets. As shown in Figure 6d, this change

https://doi.org/10.1021/acs.jpcc.1c08288
J. Phys. Chem. C 2021, 125, 27394−27402

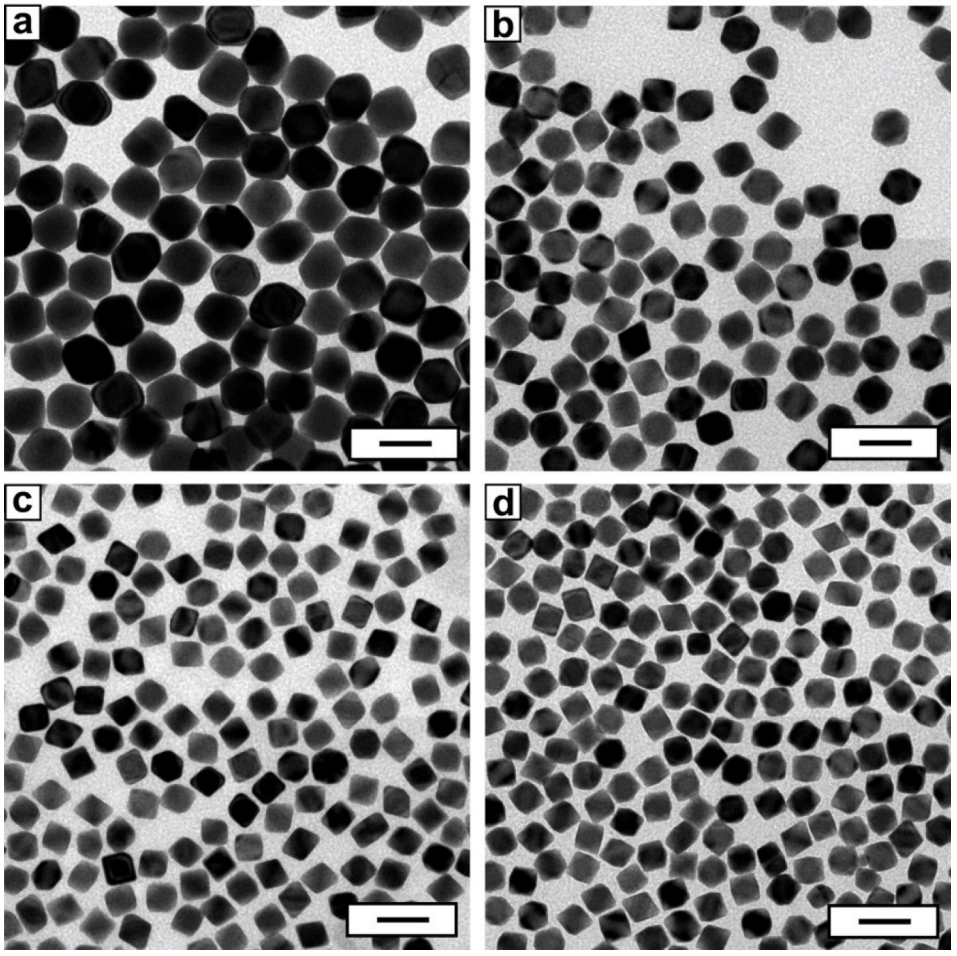

Figure 7. TEM images of the Au nanocrystals synthesized using the standard protocol except that the amount of the spherical seeds was adjusted from 10 μL to (a) 20, (b) 50, (c) 80, and (d) 100 μL, respectively. Scale bars: 50 nm.

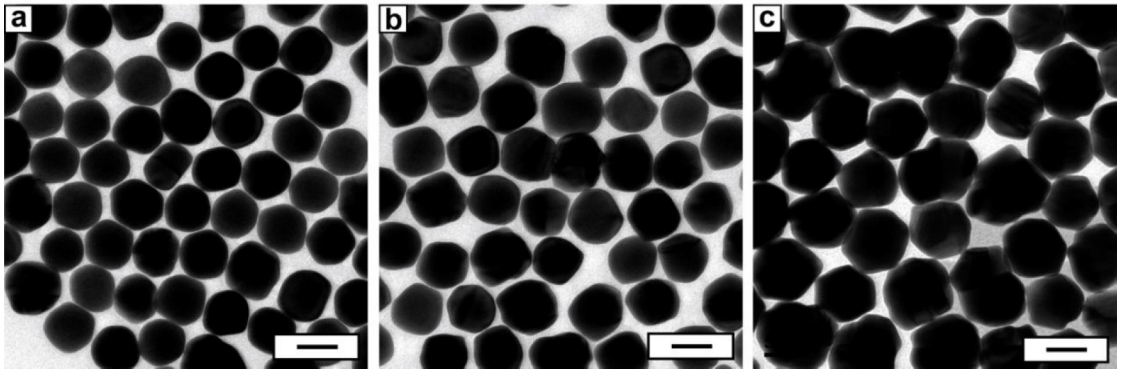

Figure 8. TEM images of the Au nanocrystals synthesized using the standard protocol except that the amount of water added into DMF was increased from 35 μL to (a) 200, (b) 500, and (c) 1000 μL, respectively. Scale bars: 50 nm.

eventually led to the formation of octahedra—a thermodynamic product, because the {111} facets have the lowest surface free energy among the low-index facets. In general, the reaction temperature affects both reduction (and thus deposition) and surface diffusion kinetics. As illustrated in Figure 3, there is an optimal temperature at which the reduction of precursor would be adequate to allow for enough deposition to balance out surface diffusion. Under this condition, the seeds are able to grow in a layer-by-layer fashion to generate AuRD with gradually enlarged sizes. If the temperature is increased, diffusion will quickly outpace deposition for the formation of a thermodynamic product. Taken together, the window for achieving a kinetic product such as RD is relatively narrow, and it critically depends on the reducing agent and temperature.

Another interesting way of altering the growth pattern and thus the outcome of a synthesis was to vary the amount of Au seeds available at the beginning of a synthesis. As the number of spherical seeds was increased, the amount of precursor allocated to each seed would decrease. The results in Figure 7

https://doi.org/10.1021/acs.jpcc.1c08288
J. Phys. Chem. C 2021, 125, 27394−27402

show that as the effective amount of precursor dropped, the synthesis trended more toward the thermodynamic, octahedral product, which is consistent with the literature on Au nanocrystal syntheses involving DMF.[14,25] As shown in Figure 7a, doubling the amount of Au seeds to 20 μL resulted in essentially random nanoparticles that show seemingly no preference for any facet. However, as the amount of Au seeds was increased to 50, 80, and 100 μL, the products were clearly dominated by octahedra with sharp corners and uniform edge lengths of 35, 29, and 27 nm, respectively (Figure 7b–d). As shown by the UV–vis spectrum in Figure S1, the LSPR peak of the Au octahedral nanocrystals was slightly blue-shifted relative to that of the AuRD. To understand the synthesis, it is important to keep in mind the importance of relative kinetics, as depicted in Figure 3. Unlike the case of raising the temperature, increasing the number of Au seeds should not affect the rate of surface diffusion. However, it reduced the amount of precursor available to each seed, decreasing the rate of deposition. As such, once an atom was deposited, even if diffusion was slow, it would still have enough time to diffuse across the surface before the next atom would be deposited, leading to the formation of a thermodynamic product.

While DMF functions primarily as a capping agent in this synthesis, it also has the potential to act as a reducing agent in the presence of water through the following reaction:

$$2HAuCl_4 + 3(CH_3)_2NCHO + 3H_2O = 2Au + 3(CH_3)_2NCOOH + 8H^+ + 8Cl^- \quad (1)$$

Note that a small amount of water was always present in the reaction because it was used as the carrier for the 10 nm Au seeds and the precursor used ($HAuCl_4{\cdot}3H_2O$) is extremely hydroscopic. Figure 8 shows TEM images of the products as the volume of water added into a standard synthesis was increased from 35 to 200, 500, and 1000 μL. Although some AuRD could still be observed at a volume of 200 μL (Figure 8a), the particles were essentially spherical in shape, which quickly became irregular or unidentifiable in Figure 8, parts b and c. In this case, the condition was no longer suitable for layer-by-layer growth due to the change in reduction rate and thus deposition rate. In general, the particles did not appear to have many well-defined facets at all. This can be attributed to the fact that DMF now also functioned as a reducing agent to significantly increase the atom deposition rate. Furthermore, the promoted generation of Cl^- ions shown in eq 1 and the presence of water would likely elicit oxidative etching. In this case, the Cl^-/O_2 pairs could oxidize the corner atoms, truncating growth at the deposition sites.[14] As a result, the formation of low energy {111} facets was stunted because of relatively fast reduction rates as both PVP and DMF now acted as reducing agents, while excess corner growth was prevented by oxidative etching. The product became dependent on the careful balance of these factors and the addition of more water would result in further unpredictable results for both particle shape and size.

CONCLUSION

We have developed a colloidal method for the synthesis of AuRD with a uniform size and in high purity. The method is simple and versatile, in addition to other merits such as high yield. The use of seed-mediated growth ensured a narrow size distribution. The edge lengths of the resultant AuRD could be tuned from 18–36 nm by varying the reaction time. In addition to RD, trisoctahedra and octahedra could be synthesized using the same protocol at either a larger amount of PVP or a higher temperature, respectively. By varying both the amount and molecular weight of the PVP involved, it became apparent that not only did PVP serve as a major reducing agent in the synthesis but also its reducing power was closely related to its concentration and molecular weight. Notably, only the increase of Au seed amount could result in a totally different reaction pathway. Through the use of a seed-mediated method, we were able to gain a better understanding of the effects of various reaction parameters on the shape evolution of the nanocrystals.

ASSOCIATED CONTENT

Supporting Information

The Supporting Information is available free of charge at https://pubs.acs.org/doi/10.1021/acs.jpcc.1c08288.

UV–vis spectra for AuRD, trisoctahedra, and octahedra (PDF)

AUTHOR INFORMATION

Corresponding Author

Younan Xia − *The Wallace H. Coulter Department of Biomedical Engineering, Georgia Institute of Technology and Emory University, Atlanta, Georgia 30332, United States; School of Chemistry and Biochemistry, Georgia Institute of Technology, Atlanta, Georgia 30332, United States;* orcid.org/0000-0003-2431-7048; Email: younan.xia@bme.gatech.edu

Authors

Xiaohuan Zhao − *The Wallace H. Coulter Department of Biomedical Engineering, Georgia Institute of Technology and Emory University, Atlanta, Georgia 30332, United States; State Key Laboratory of Supramolecular Structure and Materials, College of Chemistry, Jilin University, Changchun 130012, China*

Veronica D. Pawlik − *School of Chemistry and Biochemistry, Georgia Institute of Technology, Atlanta, Georgia 30332, United States*

Da Huo − *The Wallace H. Coulter Department of Biomedical Engineering, Georgia Institute of Technology and Emory University, Atlanta, Georgia 30332, United States*

Shan Zhou − *School of Chemistry and Biochemistry, Georgia Institute of Technology, Atlanta, Georgia 30332, United States*

Bai Yang − *State Key Laboratory of Supramolecular Structure and Materials, College of Chemistry, Jilin University, Changchun 130012, China;* orcid.org/0000-0002-3873-075X

Complete contact information is available at: https://pubs.acs.org/10.1021/acs.jpcc.1c08288

Author Contributions

¶X.Z. and V.D.P. contributed equally to this work.

Notes

The authors declare no competing financial interest.

ACKNOWLEDGMENTS

This work was supported in part by a research grant from the NSF (CHE-1804970) and start-up funds from the Georgia Institute of Technology. TEM imaging was performed at the

Georgia Tech Institute for Electronics and Nanotechnology, a member of the National Nanotechnology Coordinated Infrastructure (NNCI), which is supported by the National Science Foundation (ECCS-2025462).

REFERENCES

(1) Amendola, V.; Pilot, R.; Frasconi, M.; Maragò, O. M.; Iatì, M. A. Surface Plasmon Resonance in Gold Nanoparticles: A Review. *J. Phys.: Condens. Matter* **2017**, *29*, 203002.
(2) Murphy, C. J.; Gole, A. M.; Stone, J. W.; Sisco, P. N.; Alkilany, A. M.; Goldsmith, E. C.; Baxter, S. C. Gold Nanoparticles in Biology: Beyond Toxicity to Cellular Imaging. *Acc. Chem. Res.* **2008**, *41*, 1721−1730.
(3) Engel, S.; Fritz, E.-C.; Ravoo, B. J. New Trends in the Functionalization of Metallic Gold: From Organosulfur Ligands to N-Heterocyclic Carbenes. *Chem. Soc. Rev.* **2017**, *46*, 2057−2075.
(4) Lopez, N.; Nørskov, J. K. Catalytic CO Oxidation by a Gold Nanoparticle: A Density Functional Study. *J. Am. Chem. Soc.* **2002**, *124*, 11262−11263.
(5) Rosi, N. L.; Mirkin, C. A. Nanostructures in Biodiagnostics. *Chem. Rev.* **2005**, *105*, 1547−1562.
(6) Wu, H.-L.; Tsai, H.-R.; Hung, Y.-T.; Lao, K.-U.; Liao, C.-W.; Chung, P.-J.; Huang, J.-S.; Chen, I. C.; Huang, M. H. A Comparative Study of Gold Nanocubes, Octahedra, and Rhombic Dodecahedra as Highly Sensitive Sers Substrates. *Inorg. Chem.* **2011**, *50*, 8106−8111.
(7) Wang, D. H.; Kim, D. Y.; Choi, K. W.; Seo, J. H.; Im, S. H.; Park, J. H.; Park, O. O.; Heeger, A. J. Enhancement of Donor−Acceptor Polymer Bulk Heterojunction Solar Cell Power Conversion Efficiencies by Addition of Au Nanoparticles. *Angew. Chem., Int. Ed.* **2011**, *50*, 5519−5523.
(8) Huang, X.; El-Sayed, I. H.; Qian, W.; El-Sayed, M. A. Cancer Cell Imaging and Photothermal Therapy in the near-Infrared Region by Using Gold Nanorods. *J. Am. Chem. Soc.* **2006**, *128*, 2115−2120.
(9) Grzelczak, M.; Pérez-Juste, J.; Mulvaney, P.; Liz-Marzán, L. M. Shape Control in Gold Nanoparticle Synthesis. *Chem. Soc. Rev.* **2008**, *37*, 1783−1791.
(10) Tao, A. R.; Habas, S.; Yang, P. Shape Control of Colloidal Metal Nanocrystals. *Small* **2008**, *4*, 310−325.
(11) Xia, Y.; Xiong, Y.; Lim, B.; Skrabalak, S. E. Shape-Controlled Synthesis of Metal Nanocrystals: Simple Chemistry Meets Complex Physics? *Angew. Chem., Int. Ed.* **2009**, *48*, 60−103.
(12) Xiong, Y.; Wiley, B. J.; Xia, Y. Nanocrystals with Unconventional Shapes—a Class of Promising Catalysts. *Angew. Chem., Int. Ed.* **2007**, *46*, 7157−7159.
(13) Jeong, G. H.; Kim, M.; Lee, Y. W.; Choi, W.; Oh, W. T.; Park, Q. H.; Han, S. W. Polyhedral Au Nanocrystals Exclusively Bound by {110} Facets: The Rhombic Dodecahedron. *J. Am. Chem. Soc.* **2009**, *131*, 1672−1673.
(14) Kim, D. Y.; Im, S. H.; Park, O. O.; Lim, Y. T. Evolution of Gold Nanoparticles through Catalan, Archimedean, and Platonic Solids. *CrystEngComm* **2010**, *12*, 116−121.
(15) Qin, Y.; Lu, Y.; Yu, D.; Zhou, J. Controllable Synthesis of Au Nanocrystals with Systematic Shape Evolution from an Octahedron to a Truncated Ditetragonal Prism and Rhombic Dodecahedron. *CrystEngComm* **2019**, *21*, 5602−5609.
(16) Niu, W.; Zheng, S.; Wang, D.; Liu, X.; Li, H.; Han, S.; Chen, J.; Tang, Z.; Xu, G. Selective Synthesis of Single-Crystalline Rhombic Dodecahedral, Octahedral, and Cubic Gold Nanocrystals. *J. Am. Chem. Soc.* **2009**, *131*, 697−703.
(17) Wu, H.-L.; Kuo, C.-H.; Huang, M. H. Seed-Mediated Synthesis of Gold Nanocrystals with Systematic Shape Evolution from Cubic to Trisoctahedral and Rhombic Dodecahedral Structures. *Langmuir* **2010**, *26*, 12307−12313.
(18) Chung, P.-J.; Lyu, L.-M.; Huang, M. H. Seed-Mediated and Iodide-Assisted Synthesis of Gold Nanocrystals with Systematic Shape Evolution from Rhombic Dodecahedral to Octahedral Structures. *Chem. - Eur. J.* **2011**, *17*, 9746−9752.
(19) Kuo, B.-H.; Hsia, C.-F.; Chen, T.-N.; Huang, M. H. Systematic Shape Evolution of Gold Nanocrystals Achieved through Adjustment in the Amount of Haucl4 Solution Used. *J. Phys. Chem. C* **2018**, *122*, 25118−25126.
(20) Personick, M. L.; Langille, M. R.; Zhang, J.; Harris, N.; Schatz, G. C.; Mirkin, C. A. Synthesis and Isolation of {110}-Faceted Gold Bipyramids and Rhombic Dodecahedra. *J. Am. Chem. Soc.* **2011**, *133*, 6170−6173.
(21) Choi, K. W.; Kim, D. Y.; Zhong, X.-L.; Li, Z.-Y.; Im, S. H.; Park, O. O. Robust Synthesis of Gold Rhombic Dodecahedra with Well-Controlled Sizes and Their Optical Properties. *CrystEngComm* **2013**, *15*, 252−258.
(22) Zheng, Y.; Ma, Y.; Zeng, J.; Zhong, X.; Jin, M.; Li, Z.-Y.; Xia, Y. Seed-Mediated Synthesis of Single-Crystal Gold Nanospheres with Controlled Diameters in the Range 5−30 Nm and Their Self-Assembly Upon Dilution. *Chem. - Asian J.* **2013**, *8*, 792−799.
(23) Washio, I.; Xiong, Y.; Yin, Y.; Xia, Y. Reduction by the End Groups of Poly(Vinyl Pyrrolidone): A New and Versatile Route to the Kinetically Controlled Synthesis of Ag Triangular Nanoplates. *Adv. Mater.* **2006**, *18*, 1745−1749.
(24) Xia, X.; Xie, S.; Liu, M.; Peng, H.-C.; Lu, N.; Wang, J.; Kim, M. J.; Xia, Y. On the Role of Surface Diffusion in Determining the Shape or Morphology of Noble-Metal Nanocrystals. *Proc. Natl. Acad. Sci. U. S. A.* **2013**, *110*, 6669−6673.
(25) Kim, D. Y.; Li, W.; Ma, Y.; Yu, T.; Li, Z.-Y.; Park, O. O.; Xia, Y. Seed-Mediated Synthesis of Gold Octahedra in High Purity and with Well-Controlled Sizes and Optical Properties. *Chem. - Eur. J.* **2011**, *17*, 4759−4764.

https://doi.org/10.1021/acs.jpcc.1c08288
J. Phys. Chem. C 2021, 125, 27394−27402